

Title	Mesomorphic glass-forming ionic complex composed of a pair of cholesterol phthalate and 1-Cn-3-methylimidazolium: Phase transition and enthalpy relaxation behavior
Author(s)	NAKAJIMA, Itaru; KITAGUCHI, Taishi; SUGIMURA, Kazuki; TERAMOTO, Yoshikuni; NISHIO, Yoshiyuki
Citation	Polymer Journal (2018), 50: 899-909
Issue Date	2018-09
URL	<a href="http://hdl.handle.net/2433/241543">http://hdl.handle.net/2433/241543</a>
Right	This is the accepted manuscript of the article, which has been published in final form at <a href="https://doi.org/10.1038/s41428-018-0047-5">https://doi.org/10.1038/s41428-018-0047-5</a> .; This is not the published version. Please cite only the published version. この論文は出版社版ではありません。引用の際には出版社版をご確認ご利用ください。
Type	Journal Article
Textversion	author

1 **Mesomorphic glass-forming ionic complex composed of a pair of**  
2 **cholesterol phthalate and 1-*C<sub>n</sub>*-3-methylimidazolium: Phase transition**  
3 **and enthalpy relaxation behavior**

4  
5  
6  
7 Itaru Nakajima<sup>a</sup>, Taishi Kitaguchi<sup>a</sup>, Kazuki Sugimura<sup>a</sup>, Yoshikuni Teramoto<sup>b</sup>, and  
8 Yoshiyuki Nishio<sup>a\*</sup>

9  
10 <sup>a</sup> Division of Forest and Biomaterials Science, Graduate School of Agriculture, Kyoto  
11 University, Sakyo-ku, Kyoto 606-8502, Japan

12 <sup>b</sup> Department of Applied Life Science, Faculty of Applied Biological Sciences, Gifu  
13 University, Gifu 501-1193, Japan

14  
15 Correspondence: Professor Y. Nishio, Division of Forest and Biomaterials Science,  
16 Graduate School of Agriculture, Kyoto University, Sakyo-ku, Kyoto 606-8502, Japan.

17 E-mail: ynishio@kais.kyoto-u.ac.jp

18  
19  
20 Running head: Ionic complex of cholesterol derivative with *C<sub>n</sub>*Mim

1 **Abstract.** Ionic complexes of a mesogenic cholesterol derivative with 1-alkyl  
2 ( $C_n$ )-3-methylimidazolium ( $C_n\text{Mim}$ ) ( $n = 6\text{--}18$ ) were prepared from ethanol solutions  
3 containing an equimolar mixture of cholesterol hydrogen phthalate (CHP) and  
4 [ $C_n\text{Mim}$ ][OH]; the imidazolium hydroxide was obtained by anion exchange of  
5 [ $C_n\text{Mim}$ ][Br]. The complex samples, termed [ $C_n\text{Mim}$ ][CHP], were examined for  
6 evaluation of their thermal transition scheme. Except for two samples ( $n = 6, 8$ )  
7 showing no definite ordered phase, the complexes of  $n \geq 10$  formed a cholesteric ( $n =$   
8 10, 12) or smectic ( $n = 14\text{--}18$ ) mesophase in a considerably wide range of temperature;  
9 the wider range reflects an additional thermotropic property as salts of  $C_n\text{Mim}$  with  
10 longer alkyl chains. These fluid mesophases transformed into a mesomorphic vitreous  
11 solid without crystallization in a usual cooling process. For the glassy mesomorphic  
12 samples of selected complexes ( $n = 10, 18$ ), the enthalpy relaxation behavior was  
13 followed as a function of the aging temperature and time, and the data were analyzed in  
14 terms of a Kohlrausch-Williams-Watts type of stretched exponential equation. Quite a  
15 narrow distribution of the relaxation time was observed for the "liquid-crystalline  
16 glasses", indicating a high uniformity of the relaxation mode.

17  
18 **Keywords:** cholesterol derivative; imidazolium salt; ionic complex; phase transition;  
19 glassy liquid crystal; enthalpy relaxation

## 22 INTRODUCTION

23 Liquid-crystalline (LC) compounds of low molecular weight, which show a generally  
24 low melt viscosity, hardly vitrify and easily crystallize in a cooling process from their  
25 mesomorphic molten state. However, when the molecular weight of LC compounds is  
26 increased to ca.  $500\text{--}2000\text{ g mol}^{-1}$  with modification using a branched structure and/or  
27 multiple mesogenic moieties, the products of medium molecular weight often form a  
28 glassy LC phase,<sup>1-5</sup> as a result of suppression of the crystallizability. Such  
29 mesomorphic glass-forming compounds can be applied to optical films or core elements  
30 in displays<sup>6</sup> and other information materials,<sup>3,7</sup> owing to the temperature-dependent  
31 property of changing coloration or light transmittance. For example, the vitrifiable LC  
32 compounds are promising for a rewritable recording medium; viz., some information  
33 can be transferred mechanically, electrically or photochemically to a mesophase at a  
34 temperature above the glass transition temperature ( $T_g$ ), and, by simple cooling, it can  
35 be stored in the glassy state. The stored information can be erased, for instance, by  
36 isotropization at high temperatures, and then the second information can be written in

1 the same cycle. The vitrification phenomenon also prevails in LC polymers of higher  
2 molecular weight, and they are usable as various optical media for storing information;  
3 however, it is usually difficult to attain the fast and uniform response of the  
4 mesomorphic assembly to external stimuli, principally due to the high melt viscosity.

5 In an earlier study,<sup>8</sup> one of the authors (YN) successfully synthesized moderate  
6 molecular-weight compounds that form a glassy LC phase, without complicated  
7 procedures consuming time, namely, by a simple mixing and solvent-evaporating  
8 method. Those compounds were actually stoichiometric 1:1 complex salts composed  
9 of a cholesterol ester/aliphatic amine pair; where cholesterol hydrogen phthalate (CHP)  
10 and cholesterol hydrogen succinate (CHS) were used as the cholesterol derivative  
11 component, and a series of normal alkyl amines (*C<sub>n</sub>*-amine, *n* (carbon number) =  
12 12–18) were employed as the aliphatic amine component. The structural formulae of  
13 the constituents are shown in Figure 1. As indicated in this figure, the complexes are  
14 stabilized by ionic interaction through salt formation between the carboxylic acid of  
15 CHP (or CHS) and the amino group of *C<sub>n</sub>*-amine. After the study of thermotropic  
16 phase behavior for the complexes, we next investigated a so-called enthalpy relaxation  
17 phenomenon resulting from physical aging of vitreous solids, using "LC glasses" of  
18 CHP/*C<sub>n</sub>*-amines each having a definite molecular weight ( $\leq 800$ ).<sup>9,10</sup> It was observed  
19 that the distribution of the relaxation time of the CHP/*C<sub>n</sub>*-amine glasses was much  
20 narrower than that of conventional amorphous polymer glasses.

21  
22 << **Figure 1** >>

23  
24 In extension of the above studies, we have lately undertaken a comparative  
25 examination using similar cholesterol-based complexes prepared by altering the ionic  
26 ingredients, to find a general tendency in thermal properties and also to suggest a  
27 practical functionality for this kind of complex materials. In the present work, the  
28 previous cation component (i.e., *C<sub>n</sub>*-amine) was replaced by 1-normal alkyl  
29 (*C<sub>n</sub>*)-3-methylimidazolium cation, [*C<sub>n</sub>*Mim]<sup>+</sup>, to produce an ionic complex,  
30 [*C<sub>n</sub>*Mim][CHP] (see Figure 1). This cation is known as a representative component of  
31 ionic liquids (ILs) which have attracted a great deal of attention not only as a green  
32 solvent<sup>11,12</sup> but also as a new component of ion conductive materials.<sup>13</sup> Mesomorphic  
33 ILs that are capable of forming a LC phase have also been extensively studied over the  
34 past decades.<sup>14–16</sup> To take an advanced example of materialization, a one-dimensional  
35 ion conductive material was successfully designed by using ILs which formed a  
36 columnar LC phase.<sup>17,18</sup>

1 In this paper, we demonstrate new preparation of a LC glass-forming complex  
2 material in which the core of familiar ILs, *N*-substituted imidazolium, is incorporated.  
3 The thermotropic phase transition and enthalpy relaxation behavior of [C<sub>*n*</sub>Mim][CHP]  
4 complexes are characterized, with particular attention to the dependence on the C<sub>*n*</sub>  
5 length of the imidazolium component.

## 6 7 8 **EXPERIMENTAL PROCEDURES**

### 9 **Original materials**

10 Cholesterol hydrogen phthalate (CHP) was purchased from Tokyo Chemical Industry  
11 (Tokyo, Japan) and used after purification by recrystallization from ethanol solution.  
12 1-Bromodecane, 1-bromododecane, 1-bromotetradecane and 1-bromohexadecane were  
13 purchased from Tokyo Chemical Industry, and employed without further purification.  
14 1-Methylimidazole, 1-bromobutane, 1-bromooctane, 1-bromooctadecane, ethyl acetate,  
15 acetonitrile and ethanol (HPLC grade) were purchased from Wako Pure Chemical  
16 Industries (Osaka, Japan), and 1-bromohexane and toluene were purchased from  
17 Nacalai Tesque (Kyoto, Japan); they were all used as supplied. An ion exchange resin,  
18 Amberlite<sup>®</sup> IRA-400 (chloride form), was purchased from Sigma-Aldrich (Tokyo,  
19 Japan) and used after anion exchange from chloride to hydroxide by immersion into 1  
20 mol L<sup>-1</sup> NaOH aqueous solution.

### 21 22 **Synthesis of 1-C<sub>*n*</sub>-3-methylimidazolium bromide ([C<sub>*n*</sub>Mim][Br]; *n* = 6–18)**

23 All the *N*-substituted imidazolium salts used, [C<sub>*n*</sub>Mim][Br] (*n* = 6–18), were  
24 synthesized through *N*-alkylation/quaternization of 1-methylimidazole with different  
25 alkyl bromides by reference to the literature,<sup>19,20</sup> as follows: 1-methylimidazole (0.10  
26 mol) was dissolved in toluene (50 mL) at ambient temperature (~25 °C), and alkyl  
27 bromide (0.15 mol) was added to the solution. The mixture was stirred at 65 °C for 24  
28 h in a round-bottomed flask equipped with a reflux condenser under a dry N<sub>2</sub>  
29 atmosphere. Toluene solvent was removed by decantation (for *n* = 6 and 8) or  
30 evaporation (for *n* = 10–18), and the crude product was dissolved in acetonitrile and  
31 then dropped into ethyl acetate with vigorous stirring. After decanting of ethyl acetate,  
32 the remaining solvent was removed by heating the IL phase to 50 °C and stirring while  
33 on a vacuum line for 24 h. The salt products thus obtained were all identified as the  
34 respective objects of [C<sub>*n*</sub>Mim][Br] by <sup>1</sup>H NMR measurements (see, for example, the  
35 spectrum of [C10Mim][Br] given in Figure 4b).

## 1 Preparation of [C<sub>n</sub>Mim][CHP] complexes

2 Figure 2 shows an outline chart of the preparation route to the target complexes,  
3 [C<sub>n</sub>Mim][CHP], from [C<sub>n</sub>Mim][Br] and CHP as the starting materials.

### 4 << Figure 2 >>

5  
6  
7 By neutralizing amino acid with imidazolium hydroxide, Fukumoto *et al.*  
8 successfully prepared amino acid ionic liquid.<sup>21</sup> According to the method, we  
9 exchanged bromide ion of [C<sub>n</sub>Mim][Br] salts ( $n = 6-18$ ) to hydroxide ion ([OH]), in  
10 advance of the complexation of imidazolium cation with carboxylate anion of CHP.  
11 Each [C<sub>n</sub>Mim][Br] was dissolved in ethanol at 2 wt% with stirring at room temperature  
12 (25 °C). The [C<sub>n</sub>Mim][Br]/ethanol solutions thus prepared were each passed through  
13 a column filled with the hydroxide-exchanged Amberlite® IRA-400, and a series of  
14 [C<sub>n</sub>Mim][OH]/ethanol solutions were obtained. The absence of bromine in the latter  
15 solutions was confirmed by energy dispersive X-ray analysis. Then, a weighed  
16 amount of CHP was dissolved in each [C<sub>n</sub>Mim][OH] solution with stirring at 25 °C for  
17 24 h, so that the mixture contained equimolar quantities of COO<sup>-</sup> in CHP and  
18 imidazolium cation. The mixed solutions were each poured into a glass tray and dried  
19 at 25 °C. After further drying at 40 °C *in vacuo* for 24 h, [C<sub>n</sub>Mim][CHP] complexes  
20 were obtained as a laminate product.

## 21 Measurements

22  
23 FT-IR spectra were measured with a Shimadzu IRPrestige-21 spectrometer (Shimadzu  
24 Corporation, Kyoto, Japan). All the spectra were recorded at 20 °C in an absorption  
25 mode over a wavenumber range 400–4000 cm<sup>-1</sup> with a resolution of 4 cm<sup>-1</sup> via  
26 accumulation of 32 scans.

27 <sup>1</sup>H NMR spectra (300 MHz) were recorded using a Varian INOVA 300 apparatus  
28 (Varian, Palo Alto, CA, USA). The measurement conditions were as follows: solvent,  
29 CDCl<sub>3</sub>; solute concentration, 10 mg mL<sup>-1</sup>; internal standard, tetramethylsilane (TMS);  
30 temperature, 20 °C; number of scans, 64.

31 Polarized optical microscopy (POM) was conducted by using an Olympus  
32 microscope (BX60F5, Olympus Corporation, Tokyo, Japan) equipped with a Mettler  
33 FP82HT/FP90 hot-stage (Mettler Toledo, Tokyo, Japan). Samples were sandwiched  
34 between a slide and cover glass.

35 Differential scanning calorimetry (DSC) analyses were performed on a Seiko DSC  
36 6200/EXSTER 6000 apparatus (Seiko Instruments, Chiba, Japan). Both the

1 temperature and enthalpy readings were calibrated with an indium standard. A  
2 weighed amount of each sample (ca. 5 mg) was sealed in an aluminum pan.  
3 Thermograms were recorded at a scanning rate of 10 °C min<sup>-1</sup> for both heating and  
4 cooling scans. The measurements were made for all the [C<sub>n</sub>Mim][CHP] complexes  
5 prepared above, to establish their respective phase transition schemes. Phase transition  
6 temperature and enthalpy were determined from the peak-top position and peak area,  
7 respectively, of the relevant endo- or exothermic signal appearing in thermograms.  $T_g$   
8 was evaluated by adopting a universal method proposed by Richradson *et al.*<sup>22,23</sup> (see  
9 Supplementary Information), to minimize some kinetic effects due to the scanning rate  
10 and the conditions of pretreating the sample. In this purpose, the usual DSC output  
11 data of heat flow was converted into the corresponding relative enthalpy  $H$  and a plot of  
12  $H$  against temperature was constructed. Following that, two tangential lines were  
13 drawn on both sides of the glass transition region in the  $H$  versus temperature curve and  
14 a value of temperature at the point of intersection was read off as  $T_g$ .

15 Another series of DSC measurements was carried out for selected complexes in  
16 order to evaluate the enthalpy relaxation following aging at their mesomorphic glass  
17 state. A sequence of procedure of the relaxation measurements is summarized below  
18 (see Figure 3):

- 19 1) Heating each original sample to a temperature higher than the mesophase–isotropic  
20 phase transition temperature  $T_{M-I}$  by ca. 15 °C;
- 21 2) Cooling the isotropic sample at a rate of 10 °C min<sup>-1</sup> to a temperature ( $\approx T_g + 50$  °C)  
22 at which the sample assumes a mesomorphic fluid state;
- 23 3) Quenching the mesomorphic sample at a rate of  $\sim 90$  °C min<sup>-1</sup> to an aging  
24 temperature  $T_a$  ( $< T_g$ );
- 25 4) Aging the glassy sample at  $T_a$  over a time period  $t_a$  in the DSC cell ( $t_a < 1$  h) or in a  
26 thermo-regulated incubator (NCB-3200, Tokyo Rikakikai, Tokyo, Japan) ( $t_a \geq 1$  h);
- 27 5) Quenching the aged sample from  $T_a$  to  $-60$  °C;
- 28 6) Heating the frozen sample at a rate of 10 °C min<sup>-1</sup> from  $-60$  °C to a temperature  
29 above  $T_g$ .

30

31 << **Figure 3** >>

32

33

## 34 **RESULTS AND DISCUSSION**

### 35 **Formation of ionic complex**

36 Confirmation of ionic complex formation was made for [C<sub>n</sub>Mim][CHP] samples by <sup>1</sup>H

1 NMR and FT-IR measurements. Figure 4 illustrates a  $^1\text{H}$  NMR spectrum of  
2 [C10Mim][CHP] (part (a)) in comparison with that of [C10Mim][Br] (part (b)). The  
3 composition of this complex sample was evaluated as  $[\text{C10Mim}]/[\text{CHP}] = 0.99$  using  
4 the peak intensities of signals **a** and **e** for the C10Mim component and those of signals  
5 **3'** and **6'** for the CHP component. In a similar manner of calculation, all the samples  
6 with various alkyl chain lengths ( $n = 6\text{--}18$ ) showed a stoichiometric ratio of  
7  $[\text{C}n\text{Mim}]/[\text{CHP}] = 1.00 \pm 0.04$ . Furthermore, it was observed that the chemical shift  
8 value of an imidazolium proton (signal **d**) of  $[\text{C}n\text{Mim}][\text{CHP}]$  was always larger by ca.  
9 0.5 ppm than the corresponding value of  $[\text{C}n\text{Mim}][\text{Br}]$ . In the two spectra given in  
10 Figure 4, we find the proton signal concerned at 11.2 ppm for [C10Mim][CHP] and at  
11 10.6 ppm for [C10Mim][Br]. A similar shift of the imidazolium proton signal toward  
12 the lower magnetic field has been noted for  $[\text{C}n\text{Mim}][\text{Ac}]$  (Ac,  $\text{CH}_3\text{COO}^-$ ) prepared  
13 from  $[\text{C}n\text{Mim}][\text{Br}]$ .<sup>24,25</sup> By analogy with this, it may be inferred that the  
14  $[\text{C}n\text{Mim}][\text{CHP}]$  samples are a 1:1 type of complex compound linked through a salt  
15 formation of imidazolium carboxylate.

16  
17 << **Figure 4** >>  
18

19 Figure 5 displays FT-IR spectra of CHP, [C10Mim][CHP] and [C10Mim][Br] as  
20 reference. In the spectral data (a) of CHP *per se*, there appear a C=O stretching band  
21 at  $1701\text{ cm}^{-1}$  and a C-O stretching band at  $1310\text{ cm}^{-1}$ , both associated with a carboxylic  
22 acid dimer. The other major bands observed at  $1735$  and  $1255\text{ cm}^{-1}$  signalize the ester  
23 linkage of cholesterol with phthalic acid in CHP. In the data (b) of [C10Mim][CHP],  
24 there is no absorption signal of the carboxylic acid. Instead of this disappearance,  
25 absorption bands signaling carboxylate formation emerge at  $1590$  and  $1370\text{ cm}^{-1}$  in  
26 the spectrum (b). These pieces of evidence ensure the complete complexation between  
27 the two ionic constituents,  $[\text{C10Mim}]^+$  and  $[\text{CHP}]^-$ . Similar FT-IR observations were  
28 made for the other  $[\text{C}n\text{Mim}][\text{CHP}]$  samples. The formal feature of the complexes may  
29 be like a fatten tadpole-shape, as modeled in Figure 2; the cholesteryl group is  
30 articulated with the  $C_n$  tail through a somewhat bulky joint comprising phthaloyl and  
31 imidazolium moieties.

32  
33 << **Figure 5** >>  
34

35 **Thermal transition scheme**

36 Thermal transition behavior of CHP is well established in earlier studies.<sup>8-10</sup> The



1 transition scheme was essentially reproduced in the present DSC measurement: On  
2 heating the original crystalline CHP obtained from ethanol solution, it melted at 169 °C  
3 to transform into an isotropic liquid (I). When the molten CHP was cooled, the  
4 isotropic phase changed into a cholesteric mesophase ( $M_{Ch}$ ) at ~85 °C. Upon  
5 continued cooling of the mesomorphic CHP, it was vitrified at ca. 30 °C without  
6 crystallizing and with retaining a cholesteric planar texture. In the second heating scan,  
7 the anisotropic glass ( $G_{Ch}$ ) changed again into the fluid mesophase around 30 °C and  
8 then transformed into the isotropic liquid at ~92 °C. In the following cycles of cooling  
9 and heating, CHP showed the same enantiotropic phase behavior,  $I \leftrightarrow M_{Ch} \leftrightarrow G_{Ch}$  (see  
10 the first row of data listed in Table 1). It should be remarked here that the CHP  
11 molecules with a steroid mesogen are dimerized through dual intermolecular hydrogen  
12 bonding between the COOH groups at their terminal ends (see Figure 2), and this dimer  
13 is a structural unit involved in the observed phase behavior.

14 Similar DSC experiments were conducted for the tadpole-shaped  $[C_nMim][CHP]$   
15 complexes; the samples were all prepared as a crystalline material from ethanol solution.  
16 After isotropization of each sample by heating to a high temperature (>120 °C), the  
17 thermotropic phase behavior was evaluated in the subsequent cooling and heating cycles.  
18 The results are summarized in Table 1 and representative DSC data are compiled in  
19 Figure 6. Roughly we observed three patterns (A, B and C) of phase transition scheme,  
20 which varied depending on the alkyl chain length ( $n$ ) of  $[C_nMim]^+$ .

21  
22 << **Table 1** >>

23  
24 << **Figure 6** >>

25  
26 Pattern A refers to thermal behavior of the complexes of  $n = 6$  and 8. These  
27 samples exhibited only a glass transition ( $T_g < ca. 10$  °C) and no phase transition  
28 accompanied by an exo- or endo-thermic signal in the ordinary DSC cycles, as the  
29 evidence is illustrated for  $[C8Mim][CHP]$  in Figure 6a. Thus these complexes solely  
30 repeated the transition behavior,  $I \leftrightarrow G_A$  (amorphous glass).

31 In pattern B, two mesomorphic phases appear before glass transition in the cooling  
32 process from an isotropic molten state, and consecutive crystallization and fusion take  
33 place before isotropization in the heating process from a mesomorphic glass state.  
34 This pattern refers to thermal behavior of the complexes of  $n = 10$  and 12. Figure 6b  
35 illustrates DSC thermograms of  $[C10Mim][CHP]$ , together with supplementary POM  
36 photographic data. In the cooling scan, first the isotropic melt (I) transformed into a

1 cholesteric mesophase ( $M_{Ch}$ ) at 81 °C and then this phase partly changed into a smectic  
2 mesophase ( $M_{Sm}$ ) at 26 °C, followed by vitrification into a mesomorphic glass ( $G_{Ch/Sm}$ )  
3 at ca. 10 °C. This specification of the mesophases can be supported by the data of  
4 transition enthalpy (included in Figure 6b, left), and by the POM observations as well.  
5 In Figure 6b, right, the upper POM image shows a cholesteric planar texture and the  
6 lower image contains a battonet-like texture mingled with the planar one. In the  
7 subsequent heating scan, the anisotropic glass unfroze into a fluid mesophase ( $M_{Ch/Sm}$ )  
8 above 10 °C, and right after transition of  $M_{Ch/Sm} \rightarrow M_{Ch}$  at 32 °C, a cold crystallization  
9 occurred at 40–50 °C from the  $M_{Ch}$  state. Then the resulting crystal (K) melted in a  
10 temperature range 60–90 °C and ultimately transformed again into the isotropic fluid.  
11 Concerning [C12Mim][CHP], the scheme of “ $I \rightarrow M_{Ch} \rightarrow M_{Ch/Sm} \rightarrow G_{Ch/Sm}$ ” was also  
12 applicable to the cooling process of this sample, but, in the heating, a cold  
13 crystallization occurred at 45–65 °C from the  $M_{Ch/Sm}$  state that was unfrozen above  
14 ~13 °C from the  $G_{Ch/Sm}$  state. Following fusion at 70–90 °C of the formed crystal (K),  
15 the  $M_{Ch}$  phase was restored and it transformed into the isotropic melt at 123 °C.

16 Pattern C is classified as an enantiotropic scheme,  $I \leftrightarrow M_{Sm} \leftrightarrow G_{Sm}$ , and refers to  
17 thermal behavior of the complexes of  $n = 14–18$ . Examples of DSC thermograms are  
18 given in Figure 6c and d for [C14Mim][CHP] and [C18Mim][CHP], respectively. An  
19 isotropic liquid–mesophase transition (at  $>150$  °C) and a single glass transition ( $T_g \lesssim$   
20 5 °C) are clearly observed in both cooling and heating scans for these samples. The  
21 temperature range where the complexes are in a liquid-crystalline state is extremely  
22 wide. On examination by POM, a battonet texture (Figure 6c, right) or a fan-shaped  
23 texture (Figure 6d, right) was observed in their mesomorphic fluid states. These  
24 optical images are characteristic of the smectic type of liquid crystals. It was also  
25 perceived that the complexes generally preferred a molecular arrangement to orient  
26 perpendicular rather than parallel to the surface plane of a slide glass in the  
27 mesomorphic state. This tendency may be ascribed to a homeotropic character of the  
28  $C_n$  chain ( $n \geq 14$ ) serving as a considerably long tail of the complexes.

29 To survey the results listed in Table 1, we can make the following remarks: (1)  
30 [C $n$ Mim][CHP] complexes form a mesophase and solidify into a mesomorphic glass (or  
31 liquid-crystalline glass) upon cooling, except for the samples of  $n = 6$  and 8. However,  
32 even the latter two would intrinsically have an ability of forming a mesophase  
33 (according to quite a slower kinetics), which was suggested by microscopic observation  
34 of a feeble birefringent phase for the samples annealed at ~50 °C for more than 5 h.  
35 (2) The mesophase of [C $n$ Mim][CHP] tends to be more ordered with increasing length  
36 of the  $C_n$  chain (see  $\Delta H_{M-I}$  data in Table 1); the molecular arrangement therein is

1 dominantly cholesteric for  $n = 10$  and  $12$ , and smectic for  $n = 14$ – $18$ . (3)  $T_g$  of  
2  $[C_n\text{Mim}][\text{CHP}]$  tends to decrease with an increase in  $n$  and is always lower than that of  
3  $\text{CHP}$ . In contrast, the phase transition temperature  $T_{\text{M-I}}$  increases with increasing  $n$  ( $\geq$   
4  $10$ ). In particular, the values ( $122$ – $165$  °C) for the complexes of  $n \geq 12$  are  
5 extraordinarily high, beyond that ( $92.0$  °C) for  $\text{CHP}$ .

6 The  $C_n$ -length dependence of the thermal behavior of  $[C_n\text{Mim}][\text{CHP}]$  is roughly  
7 similar in a broad outline to that examined formerly for  $\text{CHP}/C_n$ -amine complexes.<sup>8,10</sup>  
8 In the latter system, however, the scheme of  $\text{I} \leftrightarrow \text{M}_{\text{Sm}} \leftrightarrow \text{G}_{\text{Sm}}$  (pattern C) was applicable  
9 to the complexes with  $C_n$ -amines of  $n = 10$ – $18$ , and  $\text{CHP}/C_8$ -amine provided a  
10 transition scheme of  $\text{I} \leftrightarrow \text{M}_{\text{Ch}} \leftrightarrow \text{G}_{\text{Ch}}$  while  $\text{CHP}/C_6$ -amine obeyed the scheme of  $\text{I} \leftrightarrow$   
11  $\text{G}_{\text{A}}$  (pattern A). Thus the ordered phases,  $\text{M}_{\text{Sm}}$  and  $\text{M}_{\text{Ch}}$ , were formed using relatively  
12 shorter  $C_n$  chains, compared with the situation in the  $[C_n\text{Mim}][\text{CHP}]$  system.  
13 Furthermore,  $T_{\text{M-I}}$  values (ca.  $85$ – $100$  °C)<sup>8</sup> observed for  $\text{CHP}/C_n$ -amine samples of  $n \geq$   
14  $12$  were noticeably lower than those of  $[C_n\text{Mim}][\text{CHP}]$ s with the same range of  $C_n$   
15 length and rather comparable to that of  $\text{CHP}$  *per se*. The very high  $T_{\text{M-I}}$  values of the  
16  $[C_n\text{Mim}][\text{CHP}]$  complexes might strongly reflect a thermotropic property as  
17  $N$ -substituted imidazolium IL, although there would be a contribution of an increase in  
18 the axial ratio of the mesogenic moiety of the complexes with the rigid imidazolium  
19 ring. According to literature,<sup>14,26–28</sup> salts of  $[C_n\text{Mim}]^+$  with longer alkyl chains ( $n =$   
20  $12$ – $18$ ) are usually crystalline at room temperature and often exhibit a liquid-crystalline  
21 (smectic) phase in the molten state; for instance,  $[C_n\text{Mim}][\text{Br}]$  of  $n \geq 12$  show  
22 transitions of  $\text{K} \rightarrow \text{M}_{\text{Sm}}$  at  $50$  °C or thereabouts and  $\text{M}_{\text{Sm}} \rightarrow \text{I}$  at temperatures much  
23 higher than  $100$  °C.<sup>27,28</sup>

### 24 25 **Enthalpy relaxation of mesomorphic glasses**

26 The physical aging of glassy materials, generally occurring during their annealing at  
27 temperatures lower than  $T_g$ , is interpreted as a spontaneous non-equilibrium  
28 phenomenon. More specifically, when a viscous fluid is vitrified below  $T_g$  by cooling,  
29 excess quantities of volume and enthalpy carried over in the solid should be decrease  
30 with time toward the respective equilibrium values at the aging temperature. This  
31 behavior is commonly designated as volume relaxation or enthalpy relaxation,<sup>29,30</sup> often  
32 attended by serious changes in mechanical property and endurance of the material.<sup>31–34</sup>  
33 In the present paper, our interest was focused on the enthalpy relaxation behavior of  
34 mesomorphic vitreous solids from a fundamental standpoint. The samples explored  
35 herein were the vitrified  $[C_n\text{Mim}][\text{CHP}]$ s of  $n = 10$  and  $18$  retaining cholesteric and  
36 smectic mesomorphies, respectively.

1 The enthalpy relaxation of glassy materials can be observed as an endothermic peak  
 2 in their DSC thermograms just after the onset of the glass transition when the aged  
 3 samples are heated. Figure 7 illustrates DSC thermograms obtained for the  
 4 [C18Mim][CHP] LC glass which was aged for different time periods at  $-10\text{ }^{\circ}\text{C}$ . The  
 5 enthalpy  $\Delta H$  can be evaluated from the endothermic peak area shaded in each  
 6 thermogram. Deservedly, the area increased with aging time, accompanied by a  
 7 systematic shift in the peak-top position and also in the onset point of the glass  
 8 transition to the side of higher temperature. Figure 8 collects data of the time  
 9 evolution of  $\Delta H$  for the glassy complex aged at various temperatures. The enthalpy  
 10 rose rapidly with time in a relatively early stage of the aging and eventually leveled off  
 11 to converge at an equilibrium  $\Delta H_{\infty}$ , the value of which became larger as the aging  
 12 temperature was lowered. A similar tendency of the dependence of  $\Delta H$  on aging time  
 13 ( $t_a$ ) and temperature ( $T_a$ ) was observed for the [C10Mim][CHP] LC glass.

14  
 15 << **Figure 7** >>

16  
 17 << **Figure 8** >>

18  
 19 Regression analysis of the  $\Delta H$  versus  $t_a$  plots was made by the following  
 20 Kohlrausch-Williams-Watts (KWW) type of equation with a stretched exponential  
 21 term:<sup>35</sup>

$$22 \quad \Delta H = \Delta H_{\infty} [1 - \exp\{-(t_a/\tau)^{\beta}\}] \quad (1)$$

23 where  $\tau$  is the relaxation time of enthalpy and  $\beta$  is a non-exponential parameter ( $0 < \beta \leq$   
 24  $1$ ) indicating the degree of distribution of the relaxation time. Table 2 collects values  
 25 of  $\tau$  and  $\beta$  determined by the best fitting to the  $\Delta H$  data observed for the present  
 26 complex glasses of  $n = 10$  and  $18$ .

27  
 28 << **Table 2** >>

29  
 30 In Figure 9a, the logarithmic plot of  $\tau$  against the reciprocal of aging temperature (in  
 31 K) is constructed for the two glassy complexes. For both complexes, the plot provided  
 32 a good linearity indicating applicability of the Arrhenius equation:

$$33 \quad \tau^{-1} = \tau_0^{-1} \exp [-E_a/(RT)] \quad (2)$$

34 where  $E_a$  is the activation energy for the enthalpy relaxation process in the glassy state,  
 35 and  $\tau_0^{-1}$  and  $R$  are the pre-exponential factor and the gas constant, respectively. Then  
 36 the energy  $E_a$  can be evaluated from the slope of each straight line of the plot. The

1 result of the evaluation is listed in Table 2. Figure 9b shows another plotting with  
2 ordinary logarithm of  $\tau$  against the inverse of a  $T_g$ -reduced aging temperature for the  
3 mesomorphic glasses. According to Angell,<sup>36</sup> the fragility of glassy materials is  
4 generally defined in the following way:

$$5 \quad m = d \log \tau / d(T_g/T) |_{T=T_g} \quad (3)$$

6 where  $m$  is the fragility index and its larger value denotes higher fragility. Table 2 also  
7 lists  $m$  data estimated from the slope of each Angel plot that gives linearity in Figure 9b.

8  
9 << **Figure 9** >>

10  
11 Table 2 includes results of similar relaxation analysis performed for LC glasses of  
12 CHP and CHP/ $C_n$ -amine ( $n = 10, 16, 18$ ).<sup>9,10</sup> In comparison with the previous results,  
13 the following remarks should be made on the enthalpy relaxation data for the present  
14 complex glasses:

15 (1) The parameter  $\beta$  was again of a higher value, situated at 0.90 and 0.84 on  
16 average for  $n = 10$  and 18, respectively. In principle, the extreme of  $\beta = 1$  means that  
17 there occurs just a single (or unified) relaxation mode, while, when the distribution of  
18 the relaxation time is very broad due to concurrence of many relaxation modes in the  
19 aging process,  $\beta$  assumes a much smaller value to approach zero. As can be seen from  
20 Table 2, the  $\beta$  values for the cholesterol-based LC glasses explored so far are all  
21 considerably larger than those (mostly 0.5–0.55)<sup>37</sup> reported for conventional amorphous  
22 polymers. Another notice is that the ionic complexes of CHP with  $C_n$ -amine and  
23  $C_n$ Mim provided somewhat higher  $\beta$  values relative to that (~0.7) observed for the neat  
24 CHP (dimer) system.

25 (2) The relaxation times of the [ $C_n$ Mim][CHP] glasses were roughly several to 40  
26 times longer than those of the CHP/ $C_n$ -amine glasses. Values of  $E_a$  estimated for the  
27 former glasses were higher than those for the latter ones, when compared between the  
28 samples having the same  $C_n$  length. With regard to the [ $C_n$ Mim][CHP] glasses, the  
29 bulkiness of the ionic junction involving an imidazolium moiety might lower the  
30 molecular mobility in the relaxation process. In any of the two complex series,  
31 however, the  $E_a$  values are much lower than those (426–1070 kJ mol<sup>-1</sup>)<sup>38,39</sup> reported for  
32 poly(styrene).

33 (3) The fragility index  $m$  and also  $E_a$  for the [ $C_n$ Mim][CHP] glasses decreased with  
34 an increase of the  $C_n$  length, as in the case for the CHP/ $C_n$ -amine glasses. Both the  
35 values for the two series of ionic complex were evidently lower than those for CHP *per*  
36 *se*. However, the estimations for [C10Mim][CHP] yielded somewhat larger  $m$  and  $E_a$ ,

1 each approaching the data for CHP, which may be attributable to an additional factor,  
2 i.e., the prevalence of cholesteric ordering rather than of smectic one. In any case, the  
3  $C_n$  tail of the respective cationic components exercised an effect of diluent solvent for  
4 the molecular assembly to promote cooperative motions. This should allow the glassy  
5 materials to be less fragile. Interestingly, the present result is in accordance with a  
6 general trend pointed out by Böhmer:<sup>40</sup> viz., the distribution of the relaxation time is  
7 rather wider (i.e.,  $\beta$  is lower) as the glassy material concerned is more fragile.

## 10 CONCLUSION

11 Stoichiometric 1:1 ionic complexes,  $[C_n\text{Mim}][\text{CHP}]$  ( $n = 6\text{--}18$ ), were successfully  
12 prepared from ethanol solutions containing an equimolar mixture of cholesterol  
13 hydrogen phthalate (CHP) and 1- $C_n$ -3-methylimidazolium hydroxide ( $[C_n\text{Mim}][\text{OH}]$ ).  
14 The hydroxide was derived from  $[C_n\text{Mim}][\text{Br}]$  by exchange of the anion. The  
15 structural feature of the complexes is a fatten tadpole-shape; the mesogenic cholesteryl  
16 group is articulated with the  $C_n$  tail through a bulky joint comprising phthaloyl and  
17 imidazolium moieties. Thermal properties involving liquid crystallinity of the ionic  
18 complexes were investigated in comparison with the previous result for a series of  
19  $\text{CHP}/C_n$ -amine.

20 Concerning the transition behavior after isotropizing treatment, the  $[C_n\text{Mim}][\text{CHP}]$   
21 complexes formed a mesophase and solidified into a mesomorphic glass upon cooling,  
22 except for the samples of  $n = 6$  and 8. The detected mesophase tended to be more  
23 ordered with increasing length of the  $C_n$  chain; the molecular arrangement therein was  
24 dominantly cholesteric for  $n = 10$  and 12, and smectic for  $n = 14\text{--}18$ . The values of  
25 isotropic transition point (i.e.,  $T_{\text{M-I}}$ ) observed for the samples of  $n \geq 12$  were much  
26 higher than those of  $\text{CHP}/C_n$ -amine complexes with the corresponding range of  $C_n$   
27 length. The marked elevation in  $T_{\text{M-I}}$  of the  $[C_n\text{Mim}][\text{CHP}]$  complexes can be  
28 interpreted as due to an additional thermotropy as imidazolium salts with longer  
29  $N$ -alkyl substituents.

30 For the mesomorphic glasses of  $[C_n\text{Mim}][\text{CHP}]$  ( $n = 10$  and 18), the enthalpy  
31 relaxation behavior was monitored as evolution of a DSC endothermic peak, and the  
32 data analysis was made in terms of the KWW type of stretched exponential function.  
33 Of significance was the confirmation of extremely narrow distribution of the relaxation  
34 time from the estimation of the exponent  $\beta$  close to unity. The activation energy  $E_a$  for  
35 the relaxation process and the fragility index  $m$  were also evaluated from the Arrhenius  
36 and Angell equations, respectively. The obtained  $E_a$  and  $m$  values were appreciably

1 higher compared to those for the vitreous CHP/*C<sub>n</sub>*-amine samples with the  
2 corresponding *C<sub>n</sub>* length. This indicates that the bulkiness of the ionic junction  
3 comprising the imidazolium moiety lowered the molecular mobility in the relaxation  
4 process.

5 The present study should serve as a helpful guide for designing functional LC  
6 materials possessing vitrifiability. The thermal and optical properties of the  
7 cholesterol-based complexes may be variable not only by altering a part of the ionic  
8 junction but also by modifying the alkyl tail of the counter component. In the  
9 meanwhile, the enthalpy relaxation analysis for the mesomorphic glasses provides  
10 useful information in understanding the physical aging of polymer glasses (involving  
11 both amorphous and liquid-crystalline glasses<sup>39,41</sup>). The present result would still  
12 reflect a generic property of low or medium molecular-weight compounds. In this  
13 respect, we will be required to complement further relaxation data using polymers  
14 having a similar complex structure as a pendant group; this is currently under way in  
15 our laboratory.

## 16 17 18 **ACKNOWLEDGEMENTS**

19 This work was partially financed by a Grant-in-Aid for Scientific Research (A) (No.  
20 26252025 to Y.N.) from the Japan Society for the Promotion of Science.

## 21 22 23 **CONFLICT OF INTEREST**

24 The authors declare no conflict of interest.

## 25 26 27 **REFERENCES**

- 28 1. Tsuji, K., Sorai, M. & Seki, S. New finding of glassy liquid crystal – a  
29 non-equilibrium state of cholesteryl hydrogen phthalate. *Bull. Chem. Soc. Jpn.* **44**,  
30 1452–1452 (1971).
- 31 2. Wedler, W., Demus, D., Zashke, H., Mohr, K., Schäfer, W. & Weissflog, W.  
32 Vitrification in low-molecular-weight mesogenic compounds. *J. Mater. Chem.* **1**,  
33 347–356 (1991).
- 34 3. Tamaoki, N. Cholesteric liquid crystals for color information technology. *Adv.*  
35 *Mater.* **13**, 1135–1147 (2001).
- 36 4. Chen, S. H., Shi, H., Conger, B. M., Mastrangelo, J. C. & Tsutsui, T. Novel

- 1 vitrifiable liquid crystals as optical materials. *Adv. Mater.* **8**, 998–1001 (1996).
- 2 5. Fan, F. Y., Culligan, S. W., Mastrangelo, J. C., Katsis, D., Chen, S. H. & Blanton,  
3 T. N. Novel glass-forming liquid crystals. 6. High-temperature glassy nematics.  
4 *Chem. Mater.* **13**, 4584–4594 (2001).
- 5 6. Van De Witte, P. & Lub, J. Optical components from a new vitrifying liquid  
6 crystal. *Liq. Cryst.* **26**, 1039–1046 (1999).
- 7 7. Tamaoki, N., Aoki, Y., Moriyama, M. & Kidowaki, M. Photochemical phase  
8 transition and molecular realignment of glass-forming liquid crystals containing  
9 cholesterol/azobenzene dimesogenic compounds. *Chem. Mater.* **15**, 719–726  
10 (2003).
- 11 8. Kimura, N., Takeshima, N., Nishio, Y. & Suzuki, H. Phase behavior of novel  
12 liquid-crystalline salts containing a cholesteryl group. *Mol. Cryst. Liq. Cryst.* **287**,  
13 35–45 (1996).
- 14 9. Yoshio, M., Miyashita, Y. & Nishio, Y. Enthalpy relaxation behavior of  
15 liquid-crystalline glasses of an esterified cholesterol derivative and its complex  
16 salts with aliphatic amines. *Mol. Cryst. Liq. Cryst.* **357**, 27–42 (2001).
- 17 10. Nishio, Y. & Chiba, R. Structural characteristics and novel functionalisation of  
18 liquid-crystalline polysaccharides and cholesterol derivatives. *Ekisho* **7**, 218–227  
19 (2003).
- 20 11. Welton, T. Room-temperature ionic liquids. Solvents for synthesis and catalysis.  
21 *Chem. Rev.* **99**, 2071–2083 (1999).
- 22 12. Hallett, J. P. & Welton, T. Room-temperature ionic liquids: solvents for synthesis  
23 and catalysis. 2. *Chem. Rev.* **111**, 3508–3576 (2011).
- 24 13. Armand, M., Endres, F., MacFarlane, D. R., Ohno, H. & Scrosati, B. Ionic-liquid  
25 materials for the electrochemical challenges of the future. *Nat. Mater.* **8**, 621–629  
26 (2009).
- 27 14. Binnemans, K. Ionic liquid crystals. *Chem. Rev.* **105**, 4148–4204 (2005).
- 28 15. Axenov, K. V. & Laschat, S. Thermotropic ionic liquid crystals. *Materials* **4**,  
29 206–259 (2011).
- 30 16. Goossens, K., Lava, K., Bielawski, C. W. & Binnemans, K. Ionic liquid crystals:  
31 versatile materials. *Chem. Rev.* **116**, 4643–4807 (2016).
- 32 17. Yoshio, M., Mukai, T., Ohno, H. & Kato, T. One-dimensional ion transport in  
33 self-organized columnar ionic liquids. *J. Am. Chem. Soc.* **126**, 994–995 (2004).
- 34 18. Shimura, H., Yoshio, M., Hoshino, K., Mukai, T., Ohno, H. & Kato, T.  
35 Noncovalent approach to one-dimensional ion conductors: enhancement of ionic  
36 conductivities in nanostructured columnar liquid crystals. *J. Am. Chem. Soc.* **130**,



- 1759–1765 (2008).
19. Bonhôte, P., Dias, A.-P., Papageorgiou, N., Kalyanasundaram, K. & Grätzel, M. Hydrophobic, highly conductive ambient-temperature molten salts. *Inorg. Chem.* **35**, 1168–1178 (1996).
20. Huddleston, J. G., Visser, A. E., Reichert, W. M., Willauer, H. D., Broker, G. A. & Rogers, R. D. Characterization and comparison of hydrophilic and hydrophobic room temperature ionic liquids incorporating the imidazolium cation. *Green Chem.* **3**, 156–164 (2001).
21. Fukumoto, K., Yoshizawa, M. & Ohno, H. Room temperature ionic liquids from 20 natural amino acids. *J. Am. Chem. Soc.* **127**, 2398–2399 (2005).
22. Richardson, M. J. & Savill, N. G. Derivation of accurate glass transition temperatures by differential scanning calorimetry. *Polymer* **16**, 753–757 (1975).
23. Kimura, N., Aizawa, K., Nishio, Y. & Suzuki, H. Determination of glass transition temperature by differential scanning calorimetry. *Kobunshi Ronbunshu* **53**, 866–868 (1996).
24. Vitz, J., Erdmenger, T., Haensch, C. & Schubert, U. S. Extended dissolution studies of cellulose in imidazolium based ionic liquids. *Green Chem.* **11**, 417–424 (2009).
25. Matthews, R. P., Villar-Garcia, I. J., Weber, C. C., Griffith, J., Cameron, F., Hallett, J. P., Hunt, P. A. & Welton, T. A structural investigation of ionic liquid mixtures. *Phys. Chem. Chem. Phys.* **18**, 8608–8624 (2016).
26. Bowlas, C. J., Bruce, D. W. & Seddon, K. R. Liquid-crystalline ionic liquids. *Chem. Commun.* 1625–1626 (1996).
27. Bradley, A. E., Hardacre, C., Holbrey, J. D., Johnston, S., McMath, S. E. J. & Nieuwenhuyzen. Small-angle X-ray scattering studies of liquid crystalline 1-alkyl-3-methylimidazolium salts. *Chem. Mater.* **14**, 629–635 (2002).
28. Getsis, A. & Mudring, A. -V. Imidazolium based ionic liquid crystals: structure, photophysical and thermal behaviour of  $[C_n\text{mim}]\text{Br} \cdot x\text{H}_2\text{O}$  ( $n = 12, 14$ ;  $x = 0, 1$ ). *Cryst. Res. Technol.* **43**, 1187–1196 (2008).
29. Weitz, A. & Wunderlich, B. Thermal analysis and dilatometry of glasses formed under elevated pressure. *J. Polym. Sci. Polym. Phys. Ed.* **12**, 2473–2491 (1974).
30. Cowie, J. M. G. & Ferguson, R. Physical aging studies in poly(vinyl methyl ether). 1. Enthalpy relaxation as a function of aging temperature. *Macromolecules* **22**, 2307–2312 (1989).
31. Mininni, R. M., Moore, R. S., Flick, J. R. & Petrie, S. E. B. The effect of excess volume on molecular mobility and on the mode of failure of glassy poly(ethylene

1 terephthalate). *J. Macromol. Sci. Part B* **8**, 343–359 (1973).

2 32. Cavaille, J. Y., Etienne, S., Perez, J., Monnerie, L. & Johari, G. P. Dynamic shear  
3 measurements of physical ageing and the memory effect in a polymer glass.  
4 *Polymer* **27**, 686–692 (1986).

5 33. Bauwens-Crowet, C. & Bauwens, J.-C. Annealing of polycarbonate below the  
6 glass transition temperature up to equilibrium: A quantitative interpretation of  
7 enthalpy relaxation. *Polymer* **27**, 709–713 (1986).

8 34. Struik, L. C. E. *Physical aging in amorphous polymers and other materials*.  
9 (Elsevier Scientific Pub. Co., Amsterdam, Netherland, 1978).

10 35. Williams, G. & Watts, D. C. Non-symmetrical dielectric relaxation behaviour  
11 arising from a simple empirical decay function. *Trans. Faraday Soc.* **66**, 80–85  
12 (1970).

13 36. Angell, C. A. Relaxation in liquids, polymers and plastic crystals — strong/fragile  
14 patterns and problems. *J. Non. Cryst. Solids* **131–133**, 13–31 (1991).

15 37. Yoshida, H. Enthalpy relaxation and fragility of amorphous polymers. *Kobunshi*  
16 *Ronbunshu* **53**, 874–876 (1996).

17 38. Yoshida, H. Enthalpy relaxation of polymeric glasses. *Netsu Sokutei* **13**, 191–199  
18 (1986).

19 39. Tanaka, Y. & Udagawa, H. Structural relaxation of a side-chain type liquid  
20 crystalline polymer having longer spacer chain: Analysis of enthalpy relaxation  
21 with an activation energy spectrum. *Kobunshi Ronbunshu* **66**, 463–469 (2009).

22 40. Böhmer, R. Non-linearity and non-exponentiality of primary relaxations. *J. Non.*  
23 *Cryst. Solids* **172–174**, 628–634 (1994).

24 41. Tokita, M., Funaoka, S. & Watanabe, J. Study on smectic liquid crystal glass and  
25 isotropic liquid glass formed by thermotropic main-chain liquid crystal polyester.  
26 *Macromolecules* **37**, 9916–9921 (2004).

27  
28  
29 Supplementary Information accompanies the paper on Polymer Journal website  
30 (<http://www.nature.com/pj>)

31

1 **Titles and legends to figures**

2  
3 **Figure 1** Structural formulae of the cholesterol-based ionic complexes, CHP (or  
4 CHS)/*C<sub>n</sub>*-amine (studied previously<sup>8-10</sup>) and [*C<sub>n</sub>*Mim][CHP] (targeted in the present  
5 paper).

6  
7 **Figure 2** Outline chart showing the preparation route to [*C<sub>n</sub>*Mim][CHP] samples (*n* =  
8 6–18) from [*C<sub>n</sub>*Mim][Br] and CHP.

9  
10 **Figure 3** Thermal program of the DSC measurement for enthalpy relaxation  
11 experiment. Abbreviations: *T<sub>M-I</sub>*, mesophase–isotropic phase transition temperature; *T<sub>g</sub>*,  
12 glass transition temperature; *T<sub>a</sub>*, aging temperature; *t<sub>a</sub>*, aging time.

13  
14 **Figure 4** <sup>1</sup>H NMR spectra of (a) [C10Mim][CHP] and (b) [C10Mim][Br] in CDCl<sub>3</sub>.  
15 Notations: †, proton signals in multitude from a steroid group of [CHP]<sup>−</sup> and f–n  
16 positions of [C10Mim]<sup>+</sup>; ‡, proton signals in multitude from a benzene ring of [CHP]<sup>−</sup>  
17 and b and c positions of [C10Mim]<sup>+</sup>. Peak integral values used for calculation of the  
18 complex composition (in (a)) are as follows: **a**, 42.12; **e**, 29.04; **3'**, 14.49; **6'**, 14.35.

19  
20 **Figure 5** FT-IR spectra of (a) CHP *per se*, (b) [C10Mim][CHP] and (c) [C10Mim][Br].  
21 Spectra (a) and (b) were measured by the standard KBr-pellet method. Spectrum (c)  
22 was recorded by a liquid-layer method in which the fluid sample was sandwiched  
23 between two KBr plates.

24  
25 **Figure 6** DSC thermograms and POM images of selected [*C<sub>n</sub>*Mim][CHP] samples:  
26 (a) [C8Mim][CHP]; (b) [C10Mim][CHP]; (c) [C14Mim][CHP]; (d) [C18Mim][CHP].  
27 The thermograms were all recorded at a scanning rate of 10 °C min<sup>−1</sup> after  
28 isotropization of each sample by heating to a temperature of >120 °C. POM images  
29 were captured at various temperatures in the cooling process. Particularly, the image  
30 in Figure 6c was obtained by tilting the sample slide on the POM stage.  
31 Abbreviations: K, crystal; M, mesophase; G, glassy state; A, amorphous; Ch,  
32 cholesteric; Sm, smectic.

33  
34 **Figure 7** DSC thermograms for the LC glass of [C18Mim][CHP], each obtained after  
35 aging for the indicated time period at −10 °C. The data were recorded in the heating  
36 scan at 10 °C min<sup>−1</sup>. Solid arrows indicate the onset point of the glass transition, and a

1 white arrow indicates the  $T_g$  position determined by a universal method proposed by  
2 Richardson *et al.*<sup>22,23</sup>

3

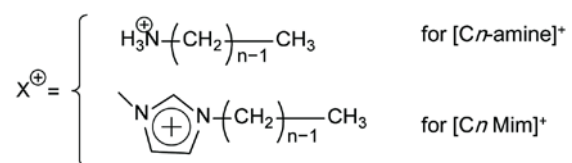
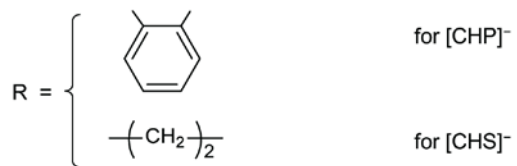
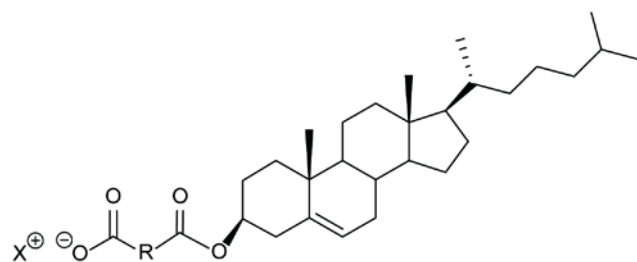
4 **Figure 8** Time evolution of enthalpy relaxation for the LC glass of [C18Mim][CHP]  
5 which was aged at different temperatures lower than  $T_g$ .

6

7 **Figure 9** (a) Arrhenius plots of the relaxation time against the reciprocal of aging  
8 temperature and (b) Angell plots of the relaxation time against the inverse of  $T_g$ -reduced  
9 aging temperature, constructed for LC glasses of [C10Mim][CHP] and  
10 [C18Mim][CHP].

11

12



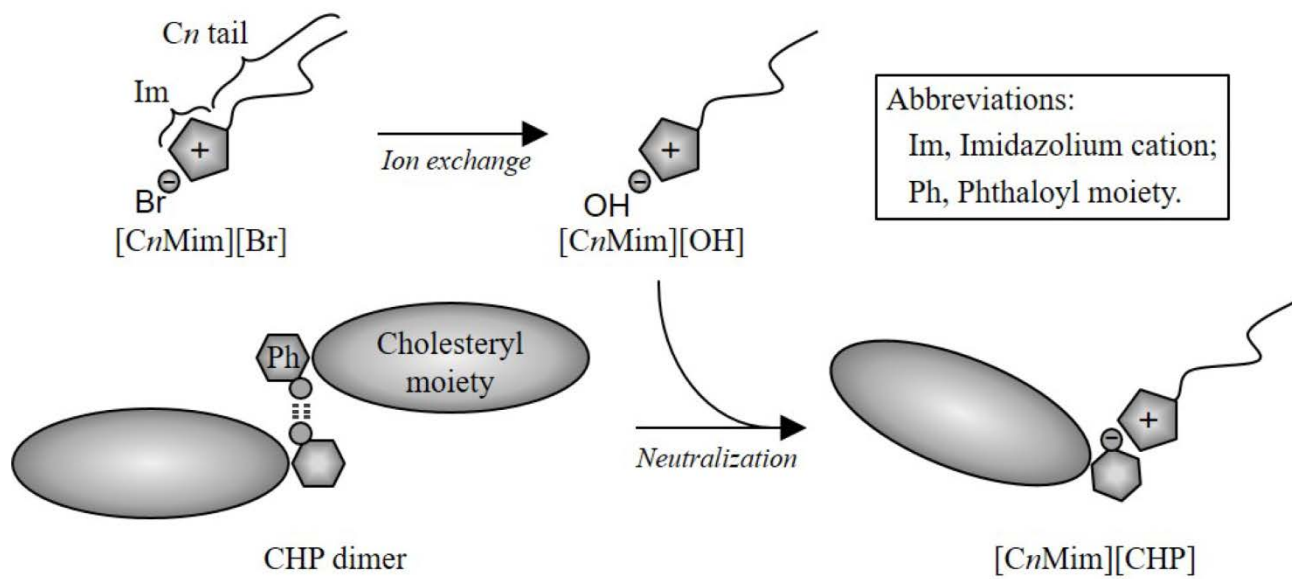
1

2

3 **Figure 1**

4

5

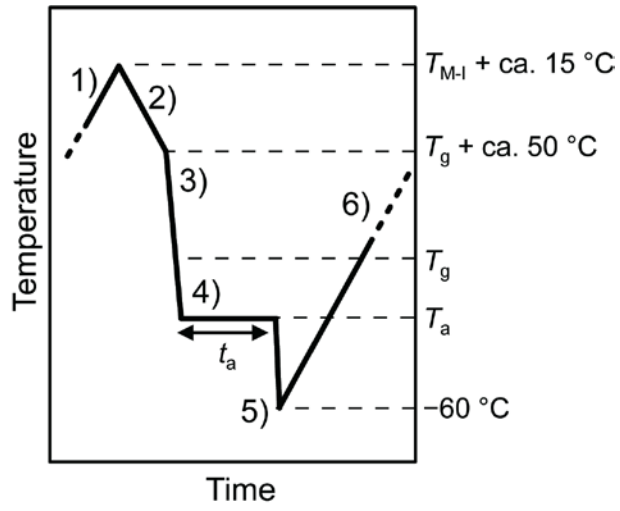


1

2 **Figure 2**

3

4

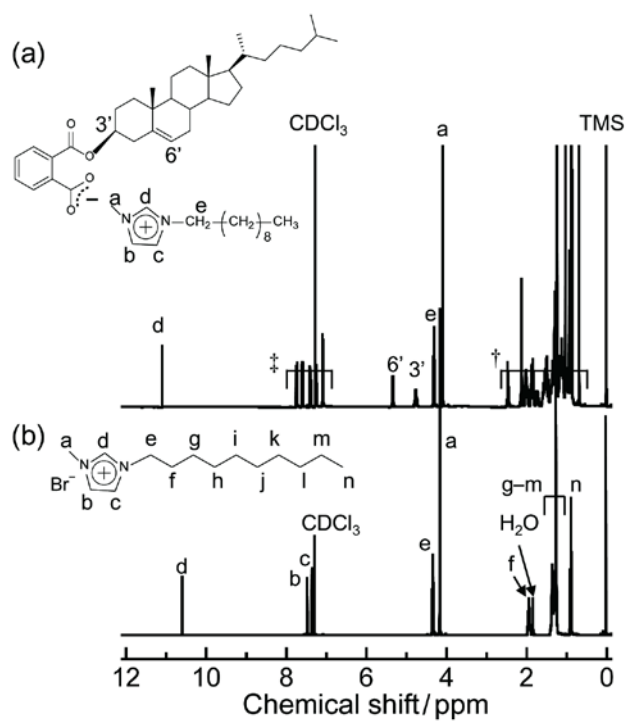


1

2 **Figure 3**

3

4



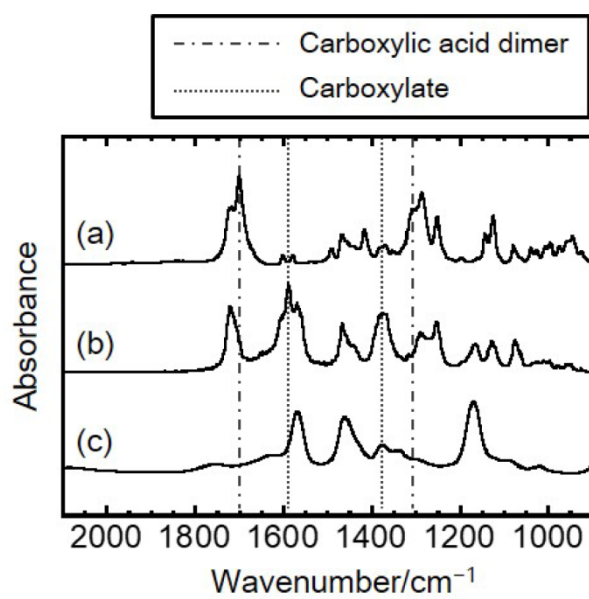
1

2 **Figure 4**

3

4



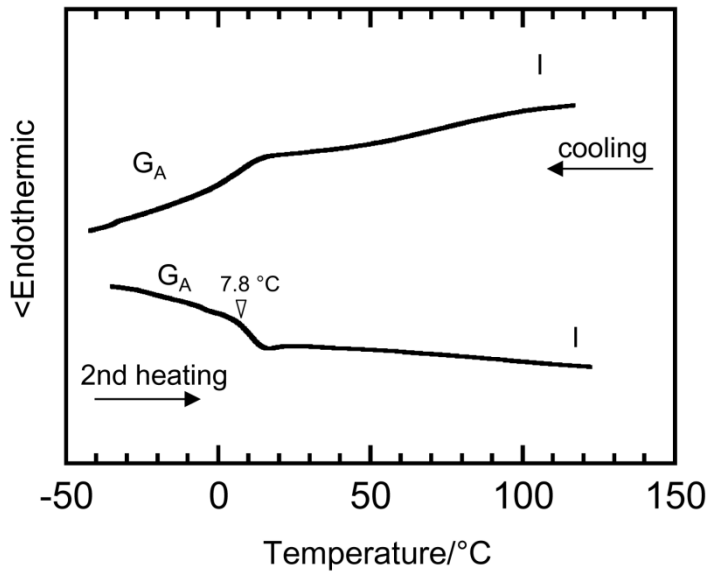


1

2 **Figure 5**

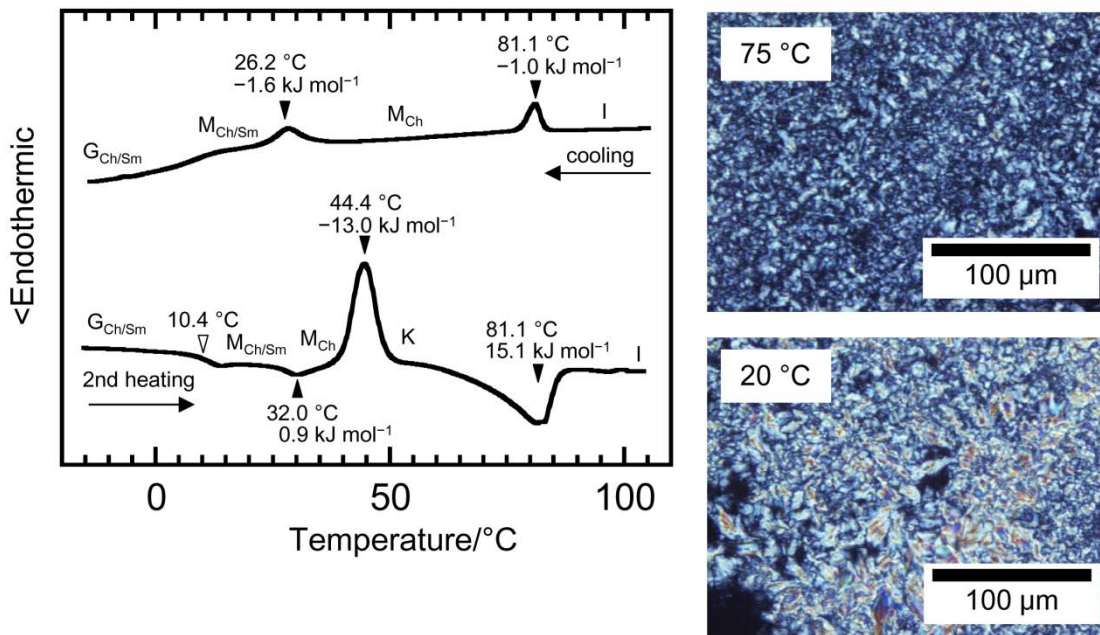
3

1 (a)



2

3 (b)



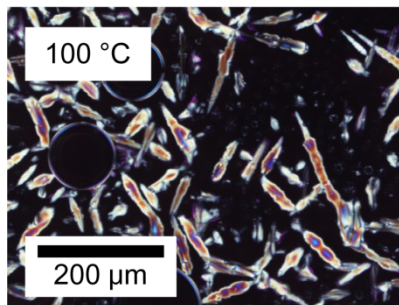
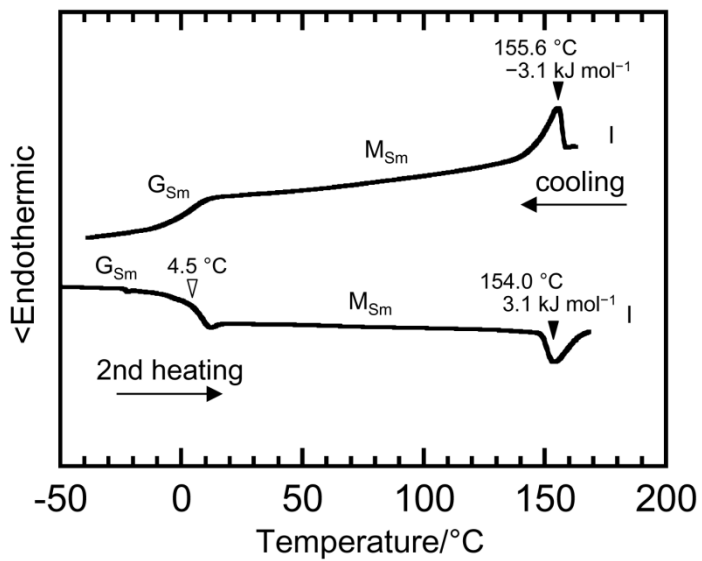
4

5

6 **Figure 6**

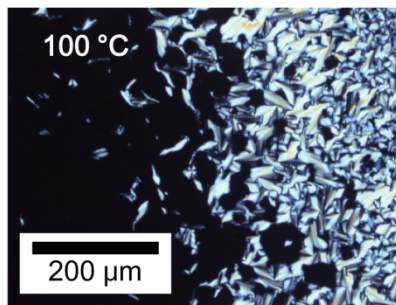
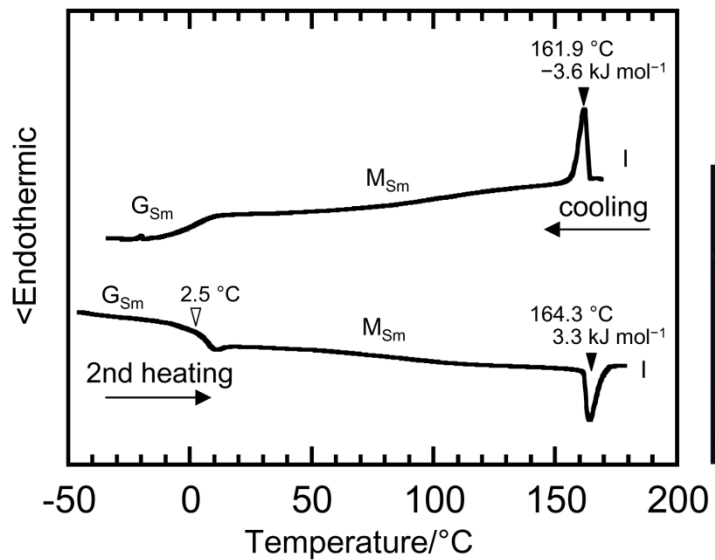
7

1 (c)



2

3 (d)

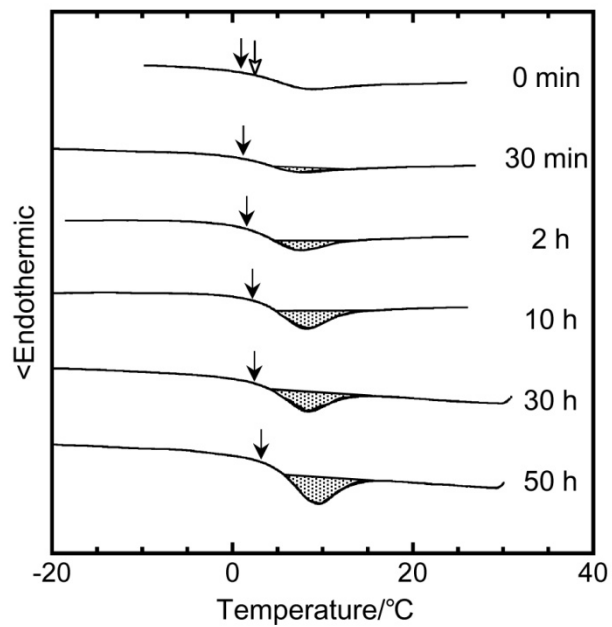


4

5 **Figure 6** Continued.

6

7

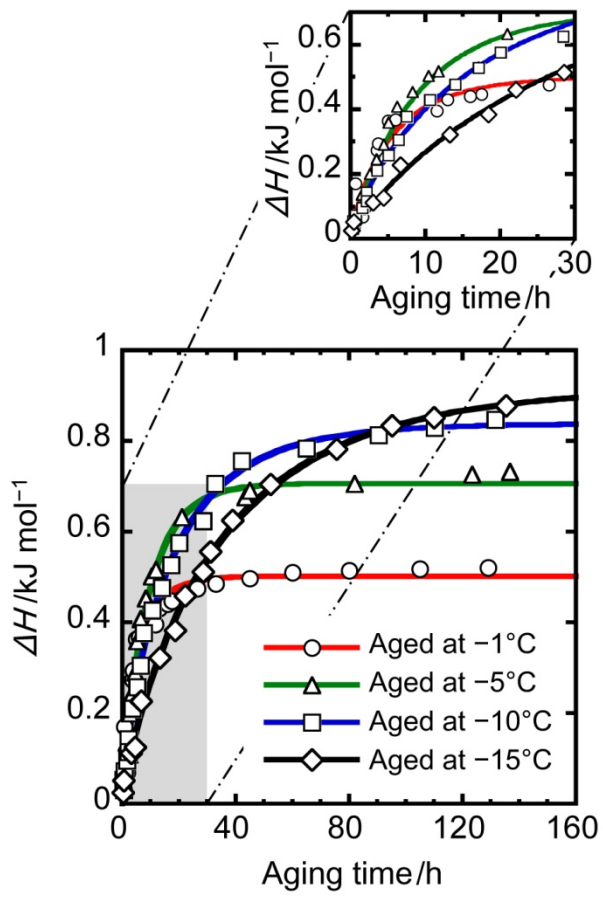


1

2 **Figure 7**

3

4

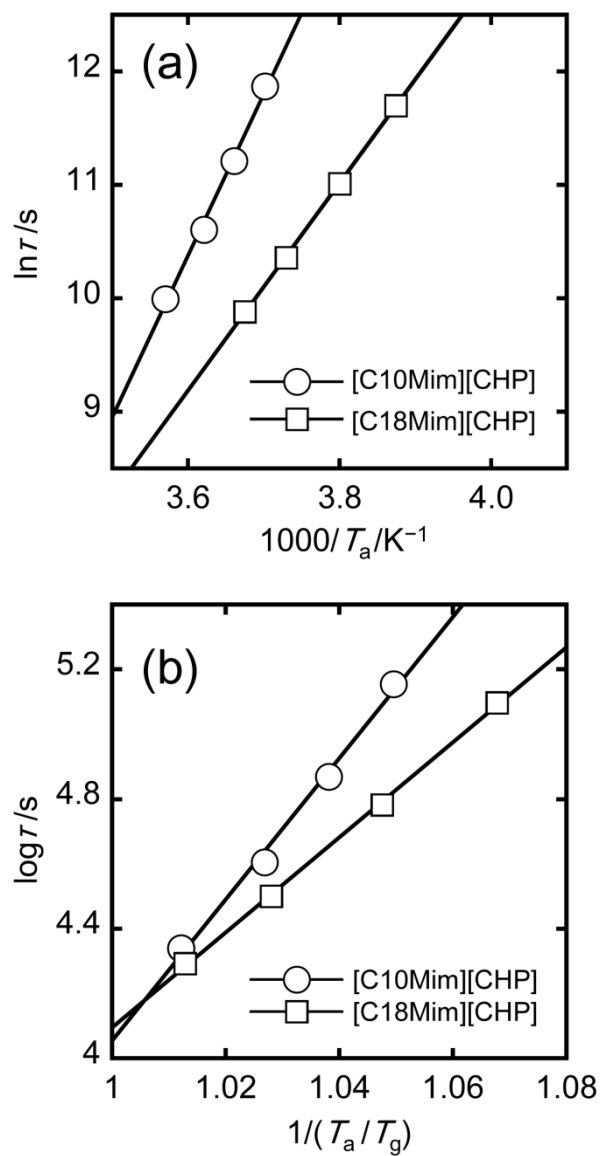


1

2 **Figure 8**

3

4



1

2 **Figure 9**

3

4

1 **Table 1** Thermal transition property of CHP and [C<sub>n</sub>Mim][CHP] complexes

2

Sample	Phase transition pattern	Phase transition scheme	T <sub>g</sub> <sup>1)</sup> /°C	T <sub>M-1</sub> <sup>1)</sup> /°C	ΔH <sub>M-1</sub> <sup>1)</sup> /kJ mol <sup>-1</sup>
CHP <i>per se</i> <sup>2)</sup>	–	G <sub>Ch</sub> ↔ M <sub>Ch</sub> ↔ I	25.8	91.4	3.3
[C6Mim][CHP]	A	G <sub>A</sub> ↔ I	13.9	–	–
[C8Mim][CHP]	A	G <sub>A</sub> ↔ I	7.8	–	–
[C10Mim][CHP]	B	$  \begin{array}{c}  G_{Ch/Sm} \leftrightarrow M_{Ch/Sm} \leftrightarrow M_{Ch} \leftrightarrow I \\  \phantom{G_{Ch/Sm} \leftrightarrow} \searrow \quad \nearrow \\  \phantom{G_{Ch/Sm} \leftrightarrow} \quad \quad \quad K  \end{array}  $	10.4	81.1	– (1.0 <sup>3)</sup> )
[C12Mim][CHP]	B	$  \begin{array}{c}  G_{Ch/Sm} \leftrightarrow M_{Ch/Sm} \leftrightarrow M_{Ch} \leftrightarrow I \\  \phantom{G_{Ch/Sm} \leftrightarrow} \searrow \quad \nearrow \\  \phantom{G_{Ch/Sm} \leftrightarrow} \quad \quad \quad K  \end{array}  $	12.6	122.6	1.7 (1.8 <sup>3)</sup> )
[C14Mim][CHP]	C	G <sub>Sm</sub> ↔ M <sub>Sm</sub> ↔ I	4.5	154.0	3.1 (3.1 <sup>3)</sup> )
[C16Mim][CHP]	C	G <sub>Sm</sub> ↔ M <sub>Sm</sub> ↔ I	4.1	161.4	3.4 (3.4 <sup>3)</sup> )
[C18Mim][CHP]	C	G <sub>Sm</sub> ↔ M <sub>Sm</sub> ↔ I	2.5	164.3	3.3 (3.6 <sup>3)</sup> )

3

4 Abbreviations: K, crystal; M, mesophase; G, glassy state; A, amorphous; Ch, cholesteric; Sm, smectic. <sup>1)</sup> Estimated in the 2nd heating scan. <sup>2)</sup> Data were all  
5 quoted from ref. 8. <sup>3)</sup> Estimated in the cooling scan.

7

8

1 **Table 2** Analytical results of enthalpy relaxation for LC glasses of CHP,  
 2 [C<sub>n</sub>Mim][CHP], and comparable CHP/C<sub>n</sub>-amine complexes

3

Sample	$T_g/^\circ\text{C}$	$T_g - T_a$ $^\circ\text{C}$	$\Delta H_\infty$ $/\text{kJ mol}^{-1}$	$\tau/\text{s}$	$\ln\tau/\text{s}$	$\beta$	$E_a$ $/\text{kJ mol}^{-1}$	$m$
CHP <i>per se</i> <sup>1)</sup>	25.8	18.8	1.83	$2.51 \times 10^5$	12.40	0.69	154	27
		10.8	1.31	$3.34 \times 10^4$	10.40	0.74		
		5.8	1.21	$1.00 \times 10^4$	9.22	0.78		
		2.8	1.02	$7.94 \times 10^3$	8.97	0.70		
[C10Mim][CHP]	10.4	13.4	1.59	$1.43 \times 10^5$	11.87	0.96	118	22
		10.4	1.44	$7.41 \times 10^4$	11.21	0.95		
		7.4	1.27	$4.04 \times 10^4$	10.61	0.87		
		3.4	1.03	$2.19 \times 10^4$	9.99	0.80		
[C18Mim][CHP]	2.5	17.5	0.919	$1.25 \times 10^5$	11.70	0.85	76	15
		12.5	0.887	$6.06 \times 10^4$	11.01	0.82		
		7.5	0.842	$3.16 \times 10^4$	10.36	0.84		
		3.5	0.502	$1.96 \times 10^4$	9.88	0.84		
CHP/C10-amine <sup>2)</sup>	18.7	16.7	1.69	$9.17 \times 10^4$	11.4	0.87	94	17
		13.7	1.52	$2.76 \times 10^4$	10.2	0.91		
		8.7	1.49	$1.77 \times 10^4$	9.78	0.98		
		3.7	1.26	$1.18 \times 10^4$	9.38	0.87		
CHP/C16-amine <sup>1)</sup>	19.0	19.0	0.849	$1.51 \times 10^3$	7.32	0.98	52	9
		14.0	0.604	$9.53 \times 10^2$	6.86	0.92		
		10.0	0.408	$7.41 \times 10^2$	6.61	0.90		
		7.0	0.262	$5.61 \times 10^2$	6.33	0.84		
CHP/C18-amine <sup>1)</sup>	20.0	25.5	0.990	$2.37 \times 10^3$	7.77	1.00	47	8
		20.3	0.949	$1.33 \times 10^3$	7.19	0.98		
		15.5	0.730	$1.04 \times 10^3$	6.95	0.91		
		13.0	0.521	$8.98 \times 10^2$	6.80	0.84		

4

5 <sup>1)</sup> Data are all quoted from ref. 9. <sup>2)</sup> Data are all quoted from ref. 10.